

# On the mechanism of the post-midnight winter $N_mF_2$ enhancements: dependence on solar activity

A. V. Mikhailov<sup>1</sup>, M. Förster<sup>2</sup>, T. Y. Leschinskaya<sup>1</sup>

<sup>1</sup> IZMIRAN, Russian Academy of Sciences, Troitsk, Russia

<sup>2</sup> Max-Planck-Institut für extraterrestrische Physik, Garching, Germany

Received: 9 February 2000 / Revised: 5 June 2000 / Accepted: 21 June 2000

**Abstract.** The mechanism of the  $N_mF_2$  peak formation at different levels of solar activity is analyzed using Millstone Hill IS radar observations. The  $h_mF_2$  nighttime increase due to thermospheric winds and the downward plasmaspheric fluxes are the key processes responsible for the  $N_mF_2$  peak formation. The electron temperature follows with the opposite sign the electron density variations in this process. This mechanism provides a consistency with the Millstone Hill observations on the set of main parameters. The observed decrease of the nighttime  $N_mF_2$  peak amplitude with solar activity is due to faster increasing of the recombination efficiency compared to the plasmaspheric flux increase. The  $\mathbf{E} \times \mathbf{B}$  plasma drifts are shown to be inefficient for the  $N_mF_2$  nighttime peak formation at high solar activity.

**Key words:** Ionosphere (ionosphere–atmosphere interactions; mid-latitude ionosphere; plasma temperature and density)

## Introduction

Nighttime  $N_mF_2$  enhancements (pre-midnight and post-midnight) are a typical phenomenon for the mid- to low-latitude  $F_2$ -region which has long been observed both in  $N_mF_2$  and TEC (Arendt and Soicher, 1964; Evans, 1965, 1974; Da Rosa and Smith, 1967; Titheridge, 1968, 1973; Bertin and Papet-Lepine, 1970; Young *et al.*, 1970; Tyagi, 1974; Davies *et al.*, 1979; Kersley *et al.*, 1980; Jakowski *et al.*, 1986, 1991; Balan and Rao, 1987; Joshi and Iyer, 1990; Jakowski and Förster, 1995). A morphological study by Mikhailov *et al.* (2000) of the  $N_mF_2$  nighttime enhancements on the latitudinal chain of the Eurasian ionosonde stations has revealed systematic

variations with season and solar activity in the occurrence probability of the peaks, their amplitude and timing. In particular, the second (post-midnight) peak shows a well-pronounced seasonal variation in the occurrence probability with the peak to be more frequent in winter compared to summer both at solar minimum and maximum. The largest amplitudes of the peak take place in winter, the amplitudes being small for other seasons. The amplitude of winter  $N_mF_2$  enhancements is larger during solar minimum compared to solar maximum. There is a tendency for the amplitude to increase with latitude. A pronounced seasonal variation in the timing of the peak occurrence is also observed with winter peaks being later than summer ones.

The revealed morphological features require physical interpretation. Fluxes of thermal plasma from the plasmasphere into the nocturnal  $F_2$ -region are considered as a commonly accepted mechanism to explain the effect (Förster and Jakowski, 1986, 1988; Jakowski and Förster, 1995). However, there are problems with model simulation of such nighttime  $N_mF_2$  increases as well as with its physical mechanism. The total flux required to produce the observed nighttime electron density increase was estimated to be  $10^9 \text{ cm}^{-2} \text{ s}^{-1}$  by Davies *et al.* (1979) for winter solar minimum conditions. Jakowski *et al.* (1991) estimated necessary fluxes as  $(3-5) \times 10^8 \text{ cm}^{-2} \text{ s}^{-1}$  for similar winter solar minimum conditions. More moderate fluxes of the order of  $(1-2) \times 10^8 \text{ cm}^{-2} \text{ s}^{-1}$  are given by Bertin and Papet-Lepine (1970), Standley and Williams (1984), and Jain and Williams (1984). Direct observations at Millstone Hill (Evans, 1974, 1975) gave plasmaspheric fluxes of the order of  $10^7-10^8 \text{ cm}^{-2} \text{ s}^{-1}$  with the most probable average nighttime value of  $3 \times 10^7 \text{ cm}^{-2} \text{ s}^{-1}$ . Although the accuracy of nighttime observations is not high when electron concentration is low (Evans *et al.*, 1978), it is difficult to consider large fluxes as real, at least during low solar activity. The scatter mentioned in the required flux estimates reflects the difference in the  $\text{O}^+$  ion recombination rates for the nighttime  $F_2$ -region accepted by different authors. Our model calculations for the January 06–12, 1997, CEDAR period, (Mikhailov and

Förster, 1999) have shown that the strong  $N_mF_2$  post-midnight enhancements observed at Millstone Hill can be explained with  $O^+$  plasmaspheric fluxes equal to  $(1-2) \times 10^8 \text{ cm}^{-2} \text{ s}^{-1}$  in accordance with the Millstone Hill IS radar observations. The variety of nighttime  $N_mF_2$  variations observed during this period was shown to reflect the balance between plasma influx and the total number of recombinations in the  $F_2$ -region ionospheric column controlled by the linear loss coefficient  $\beta = \gamma_1[N_2] + \gamma_2[O_2]$ . The efficiency of recombination strongly decreases when the  $F_2$ -layer is uplifted by the nighttime equatorward thermospheric wind and even moderate fluxes of the order of  $(1-2) \times 10^8 \text{ cm}^{-2} \text{ s}^{-1}$  from the plasmasphere appear to be sufficient to produce an essential enhancement in  $N_mF_2$ . Night-to-night variations was related in our approach with the plasma compression/decompression mechanism under the action of the observed  $\mathbf{E} \times \mathbf{B}$  drift moving plasma from higher  $L$  shells to lower ones and squeezing it into the  $F_2$ -region. In contrast, Richards *et al.* (2000) when analyzing the same January 06–12, 1997, period came to the conclusion that the nighttime plasmaspheric heat flux variation drives the nighttime ionospheric density variation. However, they could not explain the reason for night-to-night plasmaspheric heat flux variation and their calculated nighttime fluxes of  $O^+$  ions at 400 km are around  $3 \times 10^8 \text{ cm}^{-2} \text{ s}^{-1}$  being by a factor of two larger than the observed ones.

Our aim here is the further analysis of the physical mechanism responsible for the  $N_mF_2$  nighttime enhancements using Millstone Hill IS radar observations. Among many features of the  $N_mF_2$  nighttime enhancements revealed by our morphological study (Mikhailov *et al.*, 2000), the dependence of the winter post-midnight  $N_mF_2$  peak amplitude on solar activity will be analyzed.

### Morphology of the American sector

It was stressed by Mikhailov *et al.* (2000) that the results of different morphological studies of the  $N_mF_2$  nighttime enhancements in various longitudinal sectors were controversial to a great extent. This may be due to either real longitudinal differences in the occurrence of this effect, or may reflect differences in the method of analysis used. As we are considering Millstone Hill observations, an additional morphological study was made for the American sector. All available ionosonde  $f_oF_2$  observations at Boulder (40.0°N, 254.7°E,  $L = 2.3$ ) were analyzed for the years of solar maximum (1957–1959, 1968–1970, 1979–1981, 1989–1990) and solar minimum (1953–1954, 1964–1965, 1975–1976, 1985–1986) using the same method as was applied to the Eurasian sector by Mikhailov *et al.* (2000). The selected years correspond to the periods around solar maxima and minima of the last four solar cycles. The presence of nighttime peaks was checked in  $N_mF_2$  daily variations for the years in question. The absolute minimum was searched in  $N_mF_2$  values within the period after sunset to 02 LT, and this value was called  $N_{min}$ . The amplitude of the peak,  $N_{peak}/N_{min}$  and the local time of its

occurrence were found for each case. A plateau of 2–3  $N_mF_2$  hourly values was referred to as a peak with its maximum in the middle of the plateau. Several maxima are possible after midnight. Therefore, the largest post-midnight maximum was found and treated as the peak. Only quiet days with  $A_p \leq 12$  were analyzed to exclude storm effects, although nighttime  $N_mF_2$  increases are frequent during storm periods. The results of the post-midnight (second) peak occurrence are given in Fig. 1 for Boulder.

In general the results are similar to those obtained for the Eurasian sector by Mikhailov *et al.* (2000). There is a well-pronounced seasonal dependence in the occurrence probability of the peak. As with the Eurasian sector the peak is most frequent in winter (November–February, 70–80% of all quiet days), the summer probability being about 40%. Seasonal differences are larger in the Eurasian sector, (80–90% and 10–30%) for winter and summer periods, respectively. It should be stressed that the seasonal pattern is the same regardless the solar activity. This contradicts the results of Jakowski *et al.* (1991) for Havana, Cuba, who found an inversion of the seasonal pattern with the largest peak occurrence in summer at high solar activity. Similar to the Eurasian sector, the winter nighttime enhancements are the largest with amplitudes being higher during solar minimum (Fig. 1, bottom). The mechanism of this solar activity dependence for the peak amplitude is analyzed below. Like the Eurasian sector there is a clear dependence in the timing of the peak: winter peaks are later in local time than equinoctial and summer ones (Fig. 1, middle panel). This also contradicts the results of Jakowski *et al.* (1991) who revealed no seasonal variations in the timing of the peak occurrence during solar minimum and are an inverse to our results showing seasonal dependence during solar maximum with summer peaks to be the latest. Perhaps additional analysis is needed for lower-latitude stations (close to Havana, Cuba) in the American sector to clear up the reason for these differences.

Summarizing the results of the morphological study we may conclude, that there are no substantial differences between the Eurasian and the American sectors in the post-midnight peak occurrence at least for stations with  $L$ -parameter close to 3. This is important for the further analysis of the Millstone Hill ( $L = 3.13$ ) observations. We must be sure that cases of nighttime  $N_mF_2$  enhancement chosen for the analysis reflect the typical situation for the given geophysical conditions.

### Millstone Hill observations

Nighttime  $N_mF_2$  enhancements are most pronounced during winter conditions. This is the outcome of the morphological study as reviewed in the previous section. Solar activity dependence of the peak amplitude is clearly seen in the observations (Fig. 1, bottom). Therefore, three January nights with Millstone Hill IS radar observations were chosen for the analysis. Solar minimum conditions are presented by January 08, 1997,

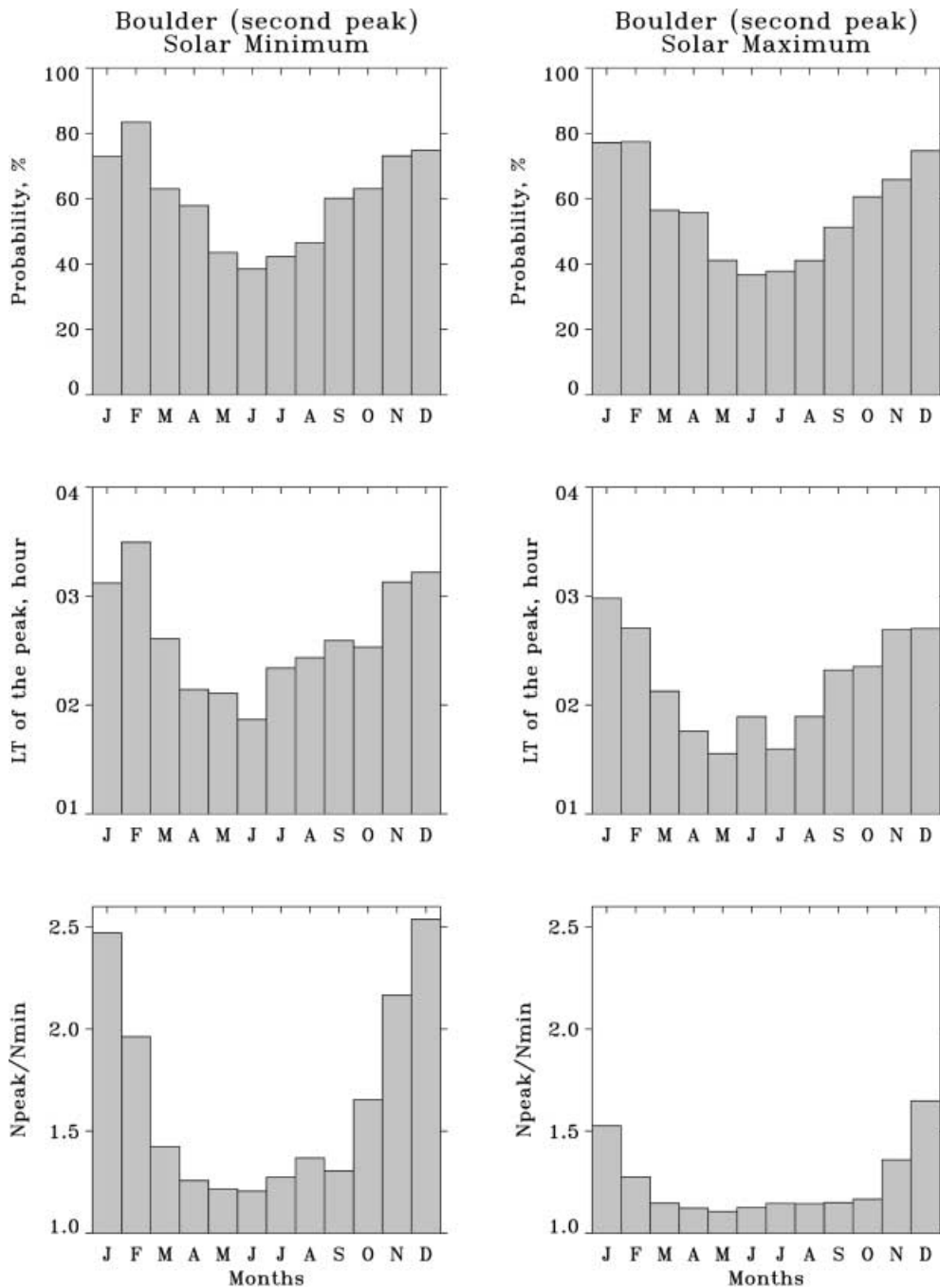


**Fig. 1.** Seasonal variations of occurrence probability (top), timing (middle), and amplitude (bottom) of the post-midnight peak in Boulder at solar minimum (left-hand side) and solar maximum (right-hand side)

( $F_{10.7} = 71.3$ ,  $\overline{F_{10.7}} = 73$ ,  $A_p = 8$ ) earlier analyzed by Mikhailov and Förster (1999), medium activity by January 24, 1993, ( $F_{10.7} = 104.8$ ,  $FS = 134.2$ ,  $A_p = 10$ ), and high solar activity by January 27, 1990, ( $F_{10.7} = 232.2$ ,  $\overline{F_{10.7}} = 200$ ,  $A_p = 4$ ), where  $\overline{F_{10.7}}$  is a 3-month average of the  $F_{10.7}$  index. Figure 2 gives the observed  $N_m F_2$  and  $h_m F_2$  nighttime variations for the dates in question. In accordance with the results of our morphological analysis the largest (by a factor of 4)  $N_m F_2$  enhancement takes place at solar minimum on January 08, 1997, the amplitude of the  $N_m F_2$  enhancement is around 2.3 on January 24, 1993, for solar medium activity and is around 1.25 only at solar maximum on January 27, 1990.

The observations selected were made using different modes. The time step was 2.5-min on January 08, 1997, a 5-min step on January 27, 1990, and a 20-min step on January 24, 1993. A “chirp correction” of  $-15.36 \text{ ms}^{-1}$  was applied to the  $V_z$  observations on January 27, 1990, while  $V_z$  values were initially corrected for the other two days. A sufficient number of observations on January 08, 1997, enabled us to calculate median plasma fluxes with SD each 15 min using a 0.5 h gate running interval, but individual  $N_e$  and  $V_z$  observations were used for the other two days. The calculated plasma fluxes are compared to the observed ones at 365 km, 406 km, and 425 km for January 08, 1997, January 24, 1993, and January 27, 1990 respectively. The choice of these

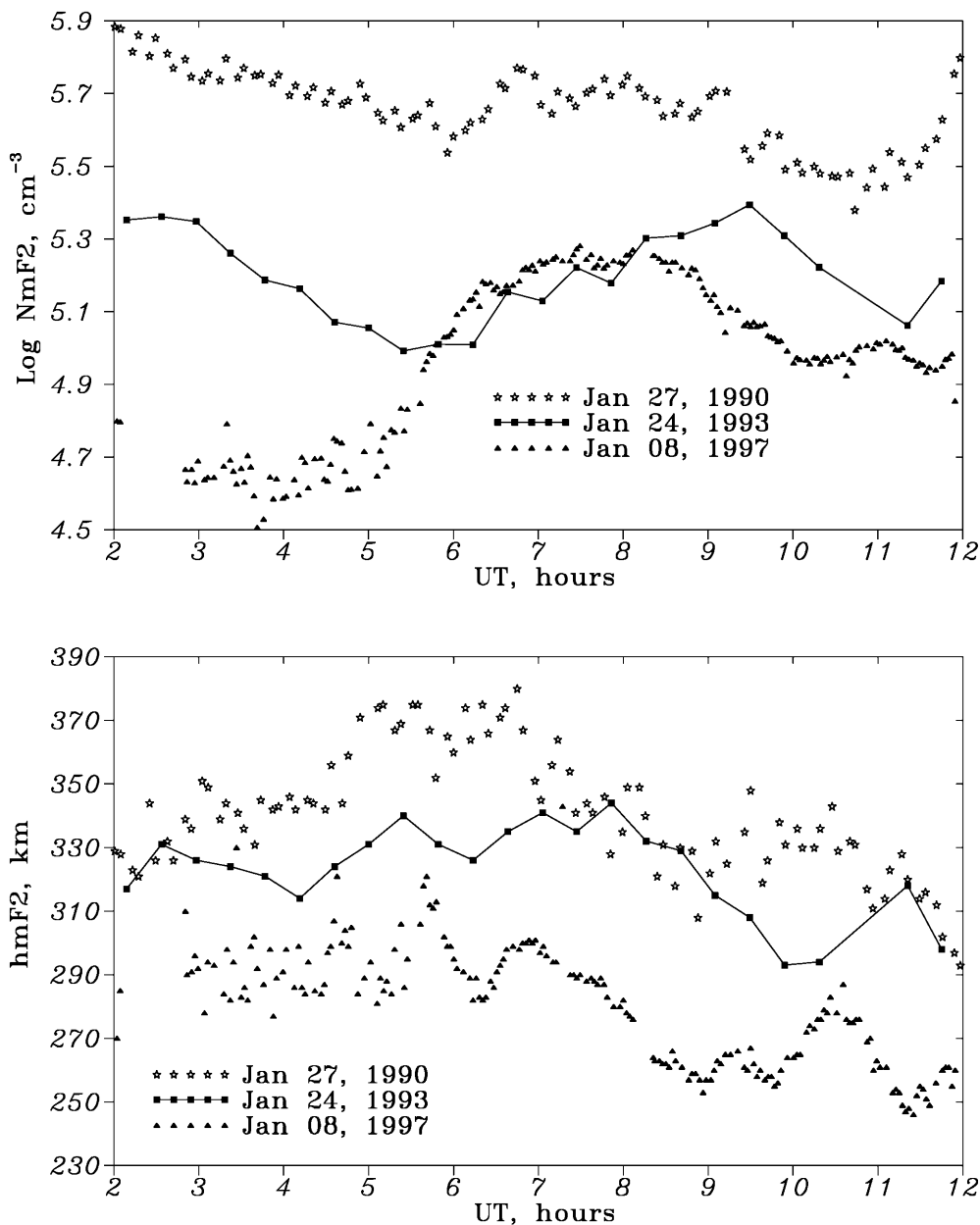


**Fig. 2.** Observed at Millstone Hill  $N_mF_2$  and  $h_mF_2$  variations for the three January nights at different levels of solar activity

heights was due to the following reasons. The level should be chosen high enough to avoid recombination effects, but the accuracy of  $V_z$  measurements strongly decreases with height. The main amount of recombinations takes place around and below  $h_mF_2$  and the experimental  $V_z$  show a large scatter and are unreliable above (depending on solar activity) 400–450 km. These factors specified the choice of the levels.

**Method of calculations**

The applied method includes two steps. First we find the thermospheric neutral composition and temperature for daytime hours to correct the MSIS-83 model values if such a correction is required. Then using these correction factors we normalize the MSIS-83 model for the nighttime hours. Usually this correction is not large for

quiet time periods analyzed here. The self-consistent method to derive thermospheric parameters from IS radar observations is described by Mikhailov and Schlegel (1997) with later modifications given by Mikhailov and Förster (1999). The main idea of the method is to fit a theoretical  $N_e(h)$  to the observed one and thus to obtain a self-consistent set of the main aeronomic parameters: neutral composition [O], [O<sub>2</sub>], [N<sub>2</sub>], temperature  $T_n(h)$ , vertical plasma drift W, and total EUV solar flux. All the parameters mentioned are responsible for the formation of the  $N_e(h)$  profile in the daytime F<sub>2</sub>-region. The theoretical model of the mid-latitude F-region used in this method is described by Förster *et al.* (1995). It takes into account transport process for O<sup>+</sup>(<sup>4</sup>S) and photo-chemical processes only for O<sup>+</sup>(<sup>2</sup>D), O<sup>+</sup>(<sup>2</sup>P), O<sub>2</sub><sup>+</sup>(X<sup>2</sup>Π), N<sup>+</sup>, N<sub>2</sub><sup>+</sup> and NO<sup>+</sup> ions in the 120–620 km height range. Vibrationally excited N<sub>2</sub> effects are not taken into account explicitly in the

model. It was shown by Mikhailov and Schlegel (2000) that recent laboratory measurements of the  $O^+ + N_2$  reaction rate constant by Hierl *et al.* (1997) could be recommended for  $F_2$ -region model calculations in the 850–1400 K temperature range. For lower temperatures the McFarland *et al.* (1973) temperature dependence may be used for this rate constant. This is important for nighttime solar minimum conditions as was shown by Mikhailov and Förster (1999). A dependence of solar EUV flux on solar activity is taken from the two-component model by Nusinov (1992) with further modifications made by Nusinov *et al.* (1999). The model is used to calculate the photo-ionization rates in 35 wavelength intervals (10–105 nm). The photo-ionization and photo-absorption cross sections are obtained mostly from Torr *et al.* (1979). Observed electron concentration at 620 km is used as the upper boundary condition to solve the continuity equation for  $O^+(^4S)$ . At the lower boundary  $O^+(^4S)$  is presumed to be in a photo-chemical equilibrium. We use the stationary form of the continuity equation for daytime hours, therefore, only periods of relative stability in  $N_mF_2$  and  $h_mF_2$  around noon are used for the analysis. Observed  $T_e(h)$  and  $T_i(h)$  profiles are used in the calculations. Collisions of  $O^+$  ions with neutral O,  $O_2$ ,  $N_2$  and  $NO^+$ ,  $O_2^+$ ,  $N_2^+$ ,  $N^+$  ions are taken into account. All  $O^+$  ion collision frequencies are taken from Banks and Kockarts (1973).

Neutral temperature  $T_n(h)$  profile and corresponding height distributions of [O],  $[O_2]$ ,  $[N_2]$  are used from the MSIS-83 model. During the fitting procedure we find factors for the initial MSIS [O],  $[O_2]$ ,  $[N_2]$  values,  $T_{ex}$  and the shape parameter  $S$  to specify the MSIS  $T_n(h)$  profile as well as a factor for the total EUV solar flux from the Nusinov (1992) model. No special constraints are laid on the searched parameters. The temperature at 120 km,  $T_{120}$  is formally added to the list of searched parameters as it was found that the method worked better if the MSIS  $T_{120}$  value was freed. Minimizing  $\Delta = [\log(N_e(h)_{obs}/N_e(h)_{cal})]^2$  in the 160–550 km height range, we find the set of thermospheric parameters in a self-consistent way.

Thermospheric parameters thus found are used to normalize the MSIS-83 model for nighttime hours. A non-stationary continuity equation for  $O^+$  ions is solved in the 150–500 km height range. Molecular  $NO^+$  and  $O_2^+$  ions are considered to be in chemical equilibrium. The  $H^+$  ions contribution may be ignored below 500 km for the conditions in question (Antonova *et al.*, 1992; MacPherson *et al.*, 1998). Model  $T_e(h)$  from Brace and Theis (1981) and  $T_i(h)$  from Banks and Kockarts (1973)

profiles are normalized at 300–400 km (depending on solar activity) by the observed values. Smoothed experimental  $h_mF_2$  values are kept by vertical plasma drift during the calculations. The profile  $N_e(h)$  observed at 0300 UT is used as the initial condition and the  $O^+$  ion flux at 500 km – as the upper boundary condition. This flux is varied to fit the observed  $N_mF_2$  variations.

## Calculations

The results of the thermospheric parameters determination for the daytime hours are given in Table 1 and they are compared there with the corresponding MSIS-83 values. Daytime observations on previous days (January 23 and January 26) are used to find the correction factors for the following nights of January 24 and January 27. The correction is not large as it is seen from Table 1. Such a correction of nighttime values by the daytime ones seems to be reasonable as we consider quiet time conditions.

The results of our calculations are given in Figs. 3–5 for the three nights in question. The figures give smoothed observed  $N_mF_2$  and  $h_mF_2$  variations, Millstone Hill estimates of neutral temperature in comparison with the used one, and the observed  $O^+$  ion fluxes compared to the calculated ones. Squares (bottom panels) are fluxes at the chosen heights obtained with the boundary fluxes required to match the observed  $N_mF_2$  variations. The boundary fluxes are generally close to those shown at the selected heights as the recombination is not very efficient above the  $F_2$ -layer maximum. Calculations were also made with constant boundary fluxes (dashes in the figures). Millstone Hill estimates of  $T_n$  were not available to the authors for January 08, 1997, therefore we used observed  $T_i$  values which are very close to  $T_n$  for the conditions in question.

The model calculations (Figs. 3–5) show that  $N_mF_2$  nighttime enhancements can be described with the  $O^+$  ion fluxes close to the observed ones at different levels of solar activity. This allows us to analyze the physical mechanism of the  $N_mF_2$  enhancement.

## Basic mechanism

Despite the variability in the post-midnight  $N_mF_2$  peak occurrence, it is possible to specify the basic mechanism responsible for the nighttime  $N_mF_2$  peak formation. This mechanism comprises the following.

**Table 1.** Calculated thermospheric parameters for the days in question. The second lines give the corresponding MSIS-83 values. LT = UT-5

Date	Time (UT)	$T_{ex}$ (K)	$T_{120}$ (K)	$lg[O]_{300}$ ( $cm^{-3}$ )	$lg[O_2]_{300}$ ( $cm^{-3}$ )	$lg[N_2]_{300}$ ( $cm^{-3}$ )	S ( $km^{-1}$ )
January 08, 1997	1700–2000	780	334	8.379	6.047	7.452	0.026
	(1830)	780	358	8.488	6.236	7.597	0.031
January 23, 1993	1700–2000	1050	351	8.740	6.720	8.042	0.023
	(1830)	978	370	8.795	6.694	8.073	0.025
January 26, 1990	1600–1800	1373	374	8.963	7.110	8.482	0.017
	(1700)	1303	388	9.065	7.166	8.538	0.019

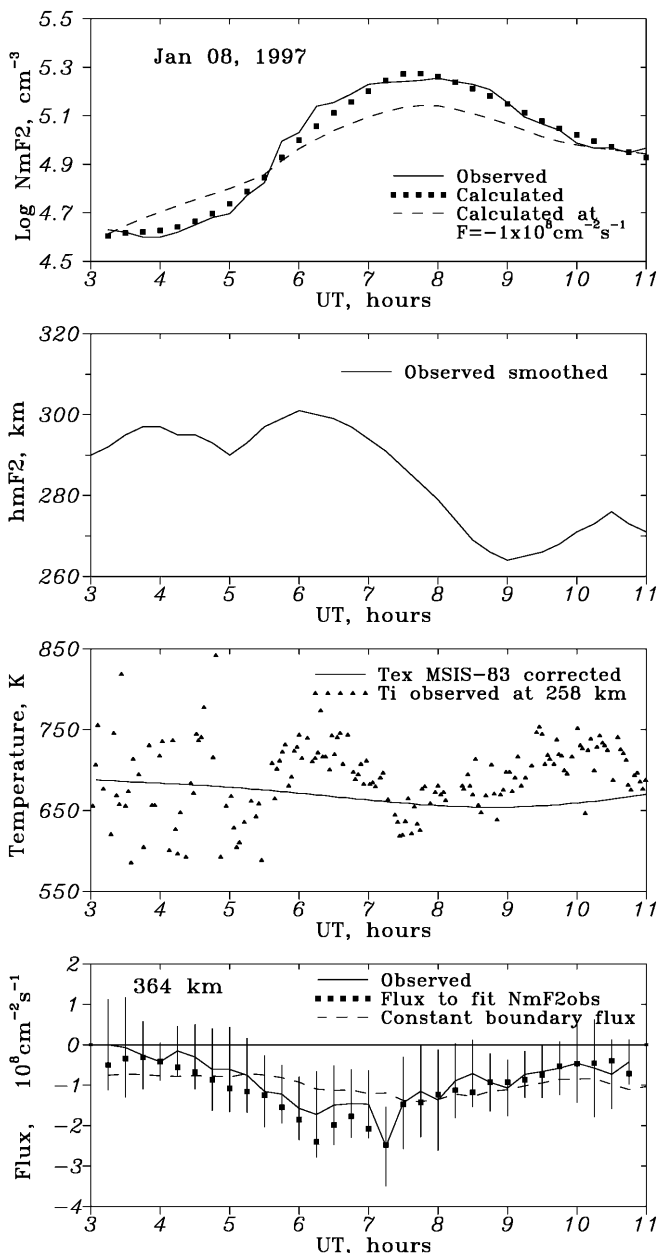


**Fig. 3.** Millstone Hill  $N_m F_2$ ,  $h_m F_2$ ,  $T_i$ , and downward  $O^+$  ion flux observations for solar minimum conditions of January 08, 1997. *Squares* calculations with the boundary flux fitting the observed  $N_m F_2$  variation, and *dashes* calculations with a constant flux  $F = -1 \times 10^8 \text{ cm}^{-2} \text{ s}^{-1}$ . A comparison with the observed fluxes is given at 364 km (see text). Note the exospheric temperature used in calculations is close to the observed  $T_i$  values, which are supposed to be close to neutral temperature for the conditions in question

1. There is always a downward  $O^+$  ions flux from the plasmasphere to the nighttime  $F_2$ -region due to plasma recombination. Vertical plasma velocity in the ambipolar case is determined by the expression (Banks and Kockarts, 1973)

$$V_z = -D_a \sin^2 I \left[ \frac{d \ln N_e}{dz} + \frac{m_i g}{k(T_e + T_i)} + \frac{d \ln(T_e + T_i)}{dz} \right] + W \quad (1)$$

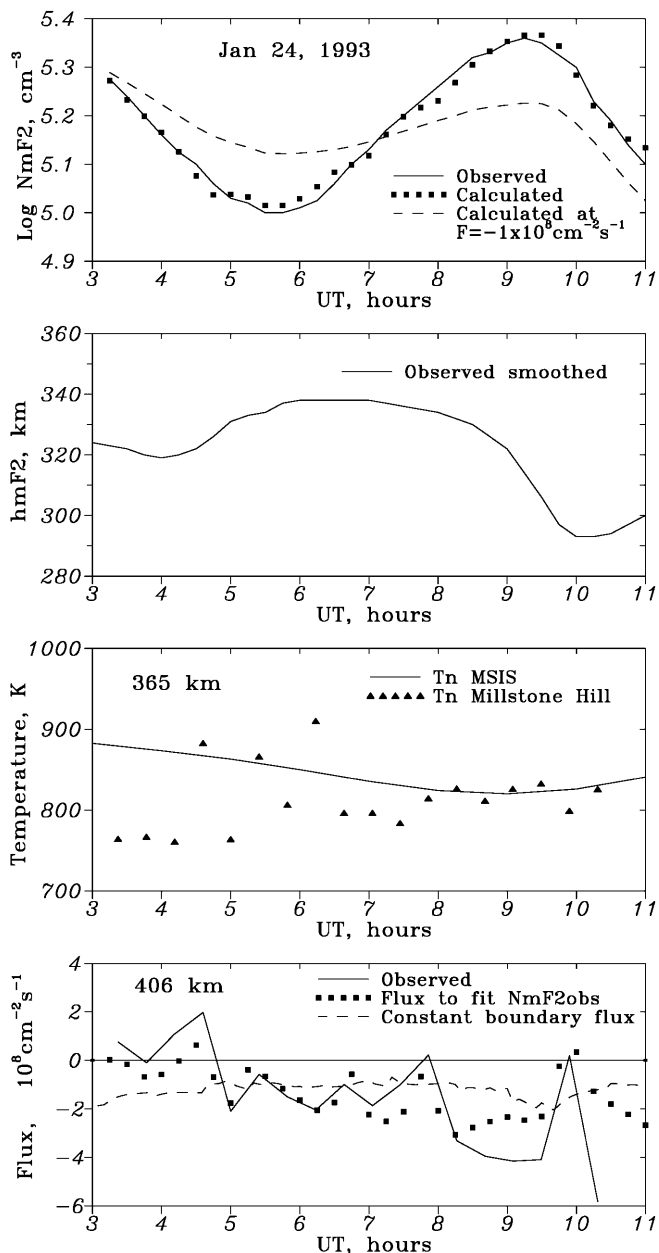


**Fig. 4.** Same as Fig. 3, but for medium solar activity of January 24, 1993. Model MSIS-83 neutral temperature used in the calculations is close to the Millstone Hill estimates of  $T_n$

where  $N_e = [O^+]$  is the electron density,  $T_e$  and  $T_i$  are the plasma temperatures,  $I$  the magnetic inclination,  $W$  the vertical plasma drift due to thermospheric winds and electric fields, and  $D_a$  the ambipolar diffusion coefficient. Expression (1) may be rewritten as

$$V_z = -D_a \sin^2 I \left[ -\frac{1}{H_{eff}} + \frac{1}{H_p} \right] + W \quad (2)$$

where

$$H_p^{-1} = \frac{m_i g}{k(T_e + T_i)} + \frac{d \ln(T_e + T_i)}{dz} \quad (3)$$

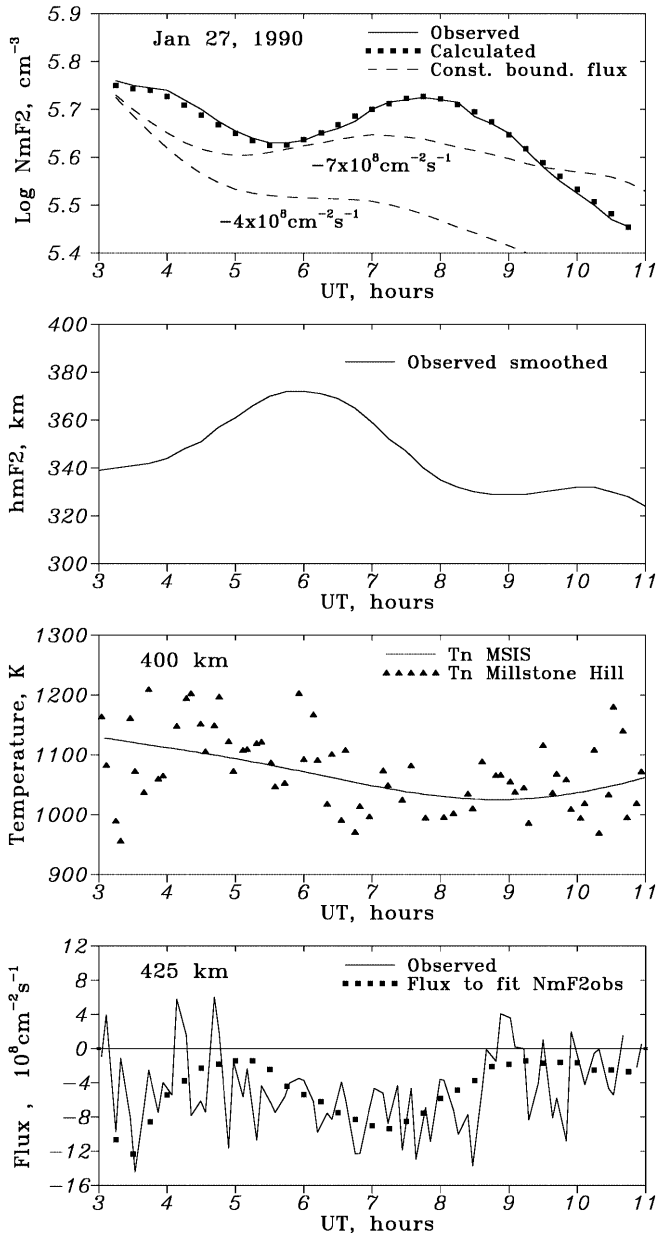


**Fig. 5.** Same as Fig. 3, but for solar maximum conditions of January 27, 1990. Calculations with two constant boundary fluxes are shown by dashes (top). Model MSIS-83 neutral temperature used in the calculations is close to the Millstone Hill estimates of  $T_n$

$$H_{eff} = -\left(\frac{d \ln N_e}{dz}\right)^{-1} \quad (4)$$

Downward plasma velocity ( $V_z < 0$ ) means  $H_{eff} > H_p$  in the topside ionosphere.

2. The starting point of the process is the increase in the meridional (equatorward) thermospheric wind velocity maximizing soon after midnight (e.g., Buonsanto and Witasse, 1999) which uplifts the  $F_2$ -layer. The  $F_2$ -layer elevation (Figs. 3–5) due to the enhanced vertical plasma drift  $W$  strongly decreases the efficiency of recombination in the  $F_2$ -layer especially at low solar activity when the thermosphere is cold

(Fig. 3) and the corresponding linear loss coefficient  $\beta = \gamma_1[N_2] + \gamma_2[O_2]$  becomes very small. For instance, on January 08, 1997, the loss coefficient  $\beta$  in the  $F_2$ -layer maximum was as small as  $1.4 \times 10^{-5} \text{ s}^{-1}$  around 07 UT.

3. With strongly decreased recombination even moderate plasmaspheric fluxes of the order of  $1 \times 10^8 \text{ cm}^{-2} \text{ s}^{-1}$  provide a sufficient plasma influx to start the electron concentration enhancement in the  $F_2$ -region.
4. The  $N_e$  increase results in the  $T_e$  decrease due to plasma cooling in the whole  $F_2$ -region. This process is clearly seen in  $N_m F_2$  and  $T_e$  variations (Figs. 3, 5 and 6).
5. The electron temperature decrease results in  $H_p$  decrease Eq. (3) and further downward plasma velocity, the  $V_z$  increase as the difference between  $H_{eff}$  and  $H_p$  becomes larger Eq. (2). This downward  $V_z$  increase is also seen in the Millstone Hill observations (Fig. 6).
6. The downward  $V_z$  increase provides additional plasma influx to the  $F_2$ -region resulting in further electron density increase and so on. This is a self-supporting avalanche type process forming the  $N_m F_2$  peak. A similar self-supporting process takes place with respect to the electron temperature leading to a steep decrease in  $T_e$  as was considered by Mikhailov and Förster (1999) for the January 06–10, 1997 CEDAR period.
7. The process stops when the equatorward  $V_{nx}$  starts to decrease later in time with a corresponding  $h_m F_2$  lowering. The  $F_2$ -layer plunges back into the high recombination region,  $N_m F_2$  starts to decrease and the described process reverses. This inversion is clearly seen in Figs. 3–6 with the decreasing  $N_m F_2$ , increasing  $T_e$  and decreasing of  $O^+$  flux. The maximal downward flux strictly coincides in time with the peak in  $N_m F_2$  variation as it is a product of  $V_z$  and  $N_e$ , both maximizing around this time.
8. According to this mechanism there should be always a delay of the  $N_m F_2$  peak with respect to the  $h_m F_2$  variation. The  $N_m F_2$  peak is to form on the slope of the lowering  $h_m F_2$ , the feature often mentioned by the authors (Evans, 1974; Mahajan and Saxena, 1976; Davies *et al.*, 1979; Jakowski *et al.*, 1991). However, it should be stressed that the beginning of the  $h_m F_2$  lowering only stops and inverts the process of the  $N_m F_2$  increasing. Therefore, it only determines the timing of the  $N_m F_2$  peak, but is not responsible for the mechanism of  $N_m F_2$  increasing. This was also mentioned by Mikhailov and Förster (1999).

#### Dependence on solar activity

According to the results of the morphological study the most pronounced solar activity effect is the decreasing of the peak amplitude with solar activity (Fig. 1). Let us analyze the results of model calculations which reproduce the observed  $N_m F_2$  variations for the three January nights belonging to different levels of solar activity. The

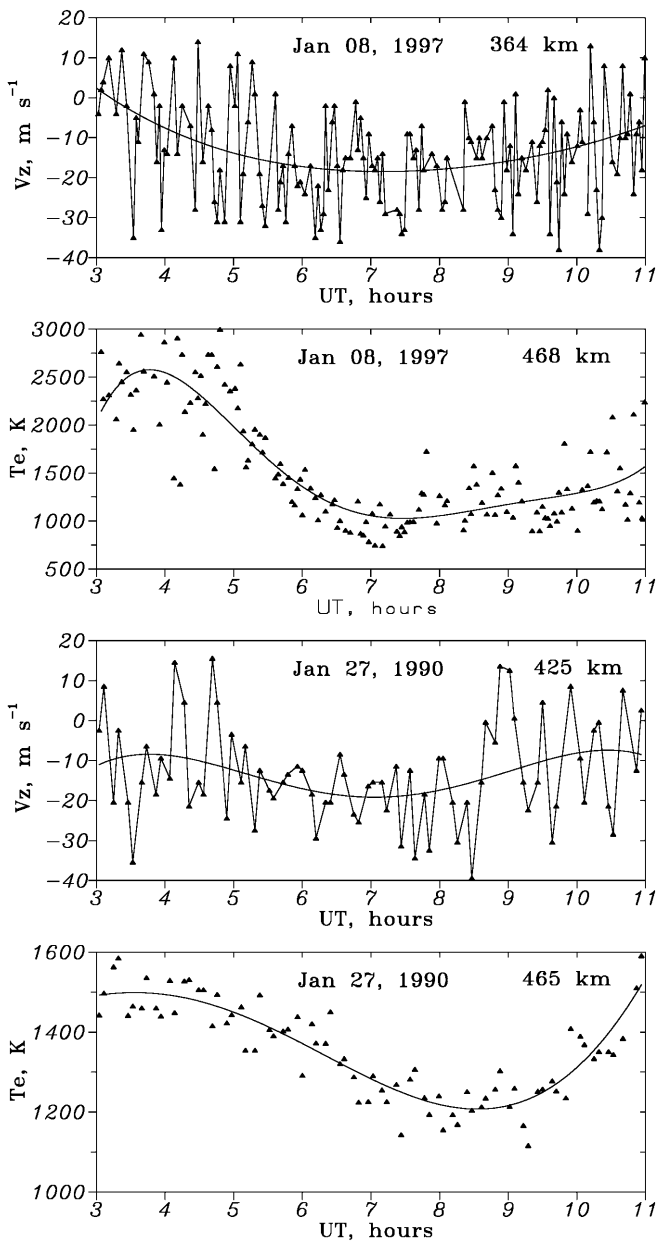


**Fig. 6.** Observed downward plasma velocity and electron temperature variations for the analyzed nights of solar minimum (January 08, 1997) and maximum (January 27, 1990) conditions. *Solid smooth curves* are polynomial least squares approximations of the observed variations which illustrate the nighttime peak  $N_m F_2$  formation mechanism (see text)

mechanism of the  $N_m F_2$  nighttime enhancement is based (as discussed already) on the balance between the total plasma influx from the plasmasphere and the total number of recombinations in the  $F_2$ -region. Table 2 gives specific (total divided by the time interval) plasma influx to the  $F_2$ -region and specific number of recombinations as well as their ratio for the three nights in question. Table 2 shows that both the specific plasma influx and the specific number of recombinations increase with solar activity, but the recombination increases faster, therefore their ratio decreases. This explains why the amplitude of the  $N_m F_2$  nighttime peak

**Table 2.** Specific plasma influx to the  $F_2$ -region and  $O^+$  ion recombinations as well as their ratio over the specified time intervals

Date Time interval	Specific plasma influx ( $\text{cm}^{-2} \text{s}^{-1}$ )	Specific number of recombinations ( $\text{cm}^{-2} \text{s}^{-1}$ )	Ratio
January 08, 1997 0400–0800 UT	$1.558 \times 10^8$	$4.989 \times 10^7$	3.124
January 24, 1993 0545–0915 UT	$2.297 \times 10^8$	$9.865 \times 10^7$	2.328
January 27, 1990 0530–0800 UT	$6.942 \times 10^8$	$5.187 \times 10^8$	1.340

decreases with solar activity. The peak value of the downward flux increases by a factor of 4 when we pass from solar minimum (Fig. 3) to solar maximum (Fig. 5) conditions. This increase is mostly due to a general increase in the electron density at high solar activity while the vertical velocities  $V_z$  are close to each other for the two nights (Fig. 6). On the other hand, the recombination efficiency increases by a factor of 10 on January 27, 1990, compared to January 08, 1997 (Table 2).

This is due to the following. At solar minimum the thermosphere is cold ( $T_{ex} \approx 700$  K, Fig. 3) while the vertical plasma drift is large ( $W \approx 60$   $\text{m s}^{-1}$ ), therefore, the  $F_2$ -layer is located in the area with low recombination, the linear loss coefficient  $\beta = \gamma_1[\text{N}_2] + \gamma_2[\text{O}_2]$  is  $1.4 \times 10^{-5} \text{ s}^{-1}$  in the  $F_2$ -layer maximum around 07 UT. At high solar activity on January 27, 1990, (Fig. 5) the neutral temperature is high ( $T_{ex} \approx 1050$  K) while the vertical plasma drift is rather small (around  $25$   $\text{m s}^{-1}$  at 08 UT) and the  $F_2$ -layer turns out to be in the relatively high recombination area ( $\beta_m = 5.3 \times 10^{-5} \text{ s}^{-1}$  at 08 UT). Therefore, available plasmaspheric fluxes can produce only small  $N_m F_2$  peaks at solar maximum conditions. The crucial point in this solar activity dependence is the decreased equatorward neutral wind which keeps the  $F_2$ -layer in the high recombination area at high solar activity. Such a dependence of the nighttime  $V_{nx}$  on the solar activity level was revealed at Millstone Hill by Buonsanto and Witasse (1999).

Although the described mechanism of the nighttime  $N_m F_2$  enhancement implies a time varying  $O^+$  ion boundary flux, the results of model calculations with a constant plasmaspheric flux may be interesting as authors usually give estimates of an average flux required to explain the observed  $N_m F_2$  enhancements. During low (Fig. 3) and moderate (Fig. 4) solar activity small plasmaspheric fluxes around  $1 \times 10^8 \text{ cm}^{-2} \text{ s}^{-1}$  are sufficient to produce a noticeable  $N_m F_2$  enhancement (dashes in Figs. 3, 4) due to the low recombination efficiency. An interesting point is that the unchanged boundary flux gives the same timing of the peak as with the time varying flux. This tells us that the timing of the peak is controlled mainly by the  $h_m F_2$  temporal variation, that is by  $V_{nx}$  and thermospheric parameter variations. At high solar activity on January 27, 1990, much stronger fluxes of about  $(7-8) \times 10^8 \text{ cm}^{-2} \text{ s}^{-1}$  are required to produce any noticeable  $N_m F_2$  peak (Fig. 5,



dashes, top) as the recombination is rather strong (see earlier). Therefore, different estimates of the required plasmaspheric flux which can be found in publications, may partly reflect different solar activity conditions analyzed by the authors.

Vertical plasma drift (due to thermospheric wind) should be strong enough to provide a sufficient  $h_mF_2$  increase and uplift the  $F_2$ -layer from the high recombination area. Figure 7 shows the case for January 28, 1990 ( $A_p = 7$ ) with a small  $h_mF_2$  excursion. The observed  $O^+$  ion flux (Fig. 7, bottom) was around  $4 \times 10^8 \text{ cm}^{-2} \text{ s}^{-1}$  which is insufficient to produce any noticeable

$N_mF_2$  enhancement at high solar activity (see earlier). A small  $h_mF_2$  increase along with small plasma influx produced only a small plateau in the  $N_mF_2$  variation around 07 UT. The basic mechanism described does not fully work in this case: only a small  $T_e$  decrease at 0630 UT without any increase in the downward plasma velocity is seen (see Fig. 6).

### Electric fields effects

Electric fields can produce a horizontal plasma transport under the action of the  $\mathbf{E} \times \mathbf{B}$  plasma drift. Thus they may contribute to the nighttime  $N_mF_2$  enhancement (Standley and Williams, 1984; Jain and Williams, 1984). Electromagnetic  $\mathbf{E} \times \mathbf{B}$  plasma drift measurements at Millstone Hill are available for the January 27–28, 1990, period analyzed. The components of the ion drifts parallel ( $V_{par}$ ) and perpendicular to the magnetic field in the northward/upward direction ( $V_{pn}$ ) at 350 km are

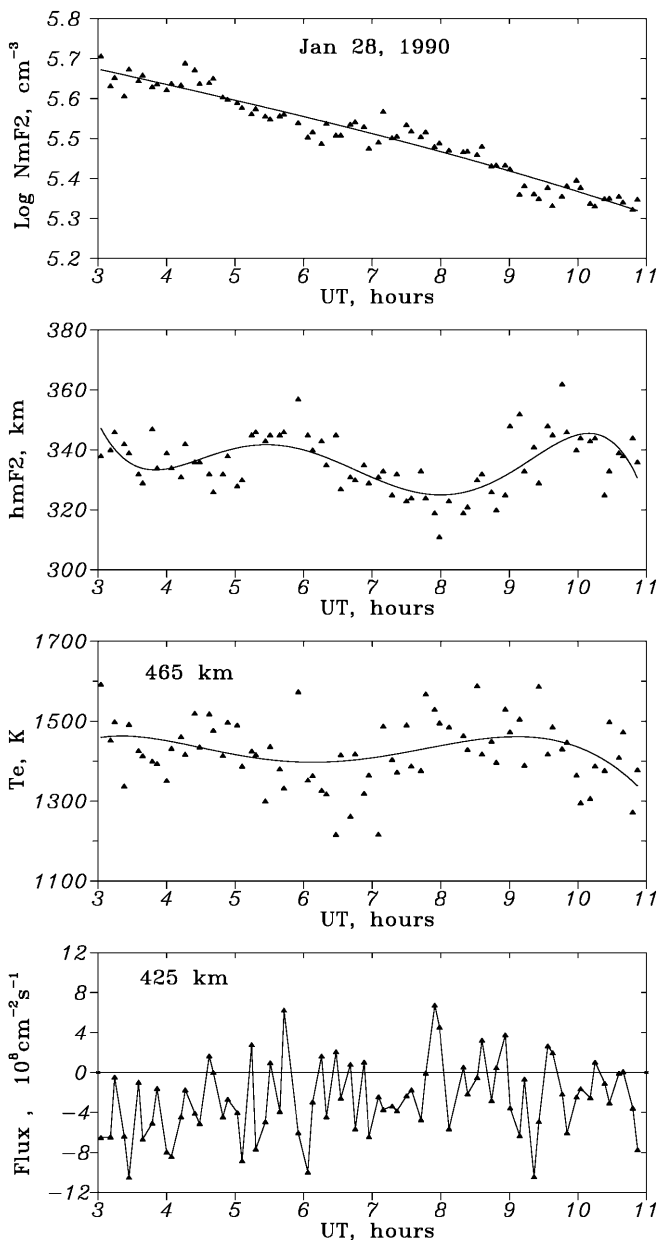


**Fig. 7.** An example of undeveloped nighttime  $N_mF_2$  enhancement on January 28, 1990 due to small  $h_mF_2$  excursion and relatively small plasmaspheric influx insufficient to produce a noticeable  $N_mF_2$  enhancement at high solar activity. *Solid smooth curves* are polynomial least squares approximations of the observed variations

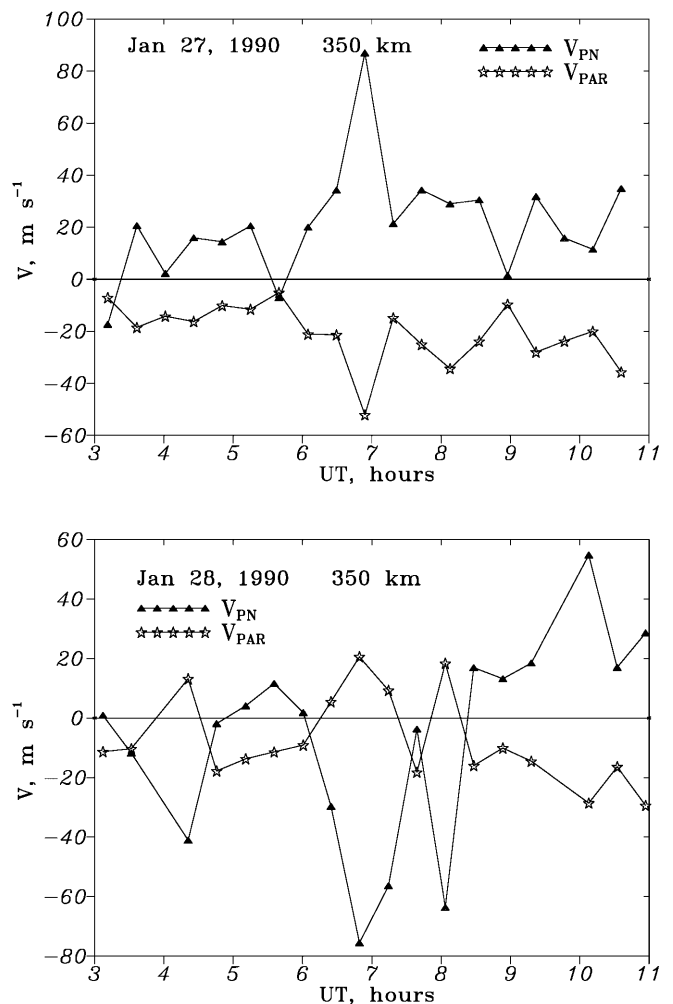


**Fig. 8.** Observed at Millstone Hill components of the ion drifts parallel ( $V_{par}$ ) and perpendicular to the magnetic field in the northward/upward direction ( $V_{pn}$ ) are shown at 350 km. Note the anticorrelations in  $V_{par}$  and  $V_{pn}$  variations resulting in mainly horizontal plasma motion which does not help in the  $F_2$ -layer uplift

shown in Fig. 8. Despite the geomagnetical quite time periods considered, strong surges in  $V_{pm}$  are seen for both nights. A well-pronounced anticorrelation between the two drift components takes place. This effect was discussed earlier by Buonsanto and Foster (1993); Buonsanto (1994) and Buonsanto and Holt (1995) as well as in the references therein. Due to this anticorrelation ionospheric plasma moves in approximately horizontal direction. This motion may result in an additional horizontal plasma influx where there are sufficiently large spatial gradients in the electron concentration. A major effect may be expected from the meridional plasma transfer due to the zonal electric field while zonal plasma transfer is much less efficient (e.g. Standley and Williams, 1984). The meridional plasma influx to the ionospheric column may be estimated as follows:

$$\begin{aligned} V_h &= - \int_z \frac{\partial N V_x}{\partial z} dz = -V_x \frac{\partial}{\partial x} \int_z N dz \\ &= -V_x \frac{\partial}{\partial x} \text{TEC} \end{aligned} \quad (5)$$

Millstone Hill ( $\Phi = 55^\circ$ ) is located on the equatorward wall of the main trough during nighttime, therefore a considerable grad(TEC) of the order of  $(2-4) \times 10^4 \text{ cm}^{-2} \text{ cm}^{-1}$  may be expected (Buonsanto, 1995; Leitinger *et al.*, 1999). Average values of  $V_{pm} = 20 \text{ ms}^{-1}$  and  $V_{par} = -20 \text{ ms}^{-1}$  may be taken throughout the whole time interval 03–11 UT for January 27, 1990 (Fig. 8). This gives a horizontal plasma velocity of  $V_x = V_{pm} \sin I - V_{par} \cos I \approx 26 \text{ m s}^{-1}$  with the Millstone Hill inclination  $I = 70^\circ$ . The resultant plasma influx  $Fh$  is around  $(5-10) \times 10^7 \text{ cm}^{-2} \text{ s}^{-1}$  depending on the assumed latitudinal grad(TEC). This is much less compared to the specific plasmaspheric influx for this date (Table 2). The peak values of  $V_{pm} = 80 \text{ m s}^{-1}$  and  $V_{par} = -50 \text{ m s}^{-1}$  (Fig. 8) give  $V_x \approx 90 \text{ m s}^{-1}$  and this could result in a considerable plasma influx comparable with the plasmaspheric one. However the duration of these surges of velocity are too short (about 1 h) to provide any noticeable changes in the electron density. The characteristic horizontal scale is more than 1000 km for the observed latitudinal grad TEC and with the  $V_x$  of  $90 \text{ ms}^{-1}$  the required characteristic time of such  $V_{pm}$  upsurges should be about 3 h i.e. much longer than the observed one. The inclusion of such a horizontal plasma transport with the observed  $V_{pm}$  and  $V_{par}$  variations to the model confirmed the low efficiency of this process. Therefore, the main source of plasma to provide the  $N_mF_2$  nighttime enhancement is the downward flux from the plasmasphere. The same conclusion was obtained by Jain and Williams (1984) by analyzing the St. Santin nighttime observations.

## Discussion

The proposed mechanism of the winter nighttime  $N_mF_2$  enhancement formation based on the analysis of our model calculations is consistent with the Millstone Hill

observations on the set of main parameters. The observed  $N_mF_2$  enhancements observed at different levels of solar activity are reproduced quantitatively in our model calculations with  $O^+$  fluxes close to the observed ones. The  $N_mF_2$  peak occurrence on the slope of the decreasing  $h_mF_2$  usually mentioned in publications is explained within the scope of this mechanism. The mechanism explains also the observed maximum in the downward plasma velocity  $V_z$  (and in the  $O^+$  flux, correspondingly) coinciding in time with the  $N_mF_2$  peak. In this mechanism the electron temperature variation is dependent on the electron density variation contrary to the approach by Richards *et al.* (2000), where the plasmaspheric heat flux variation drives the nighttime ionospheric density variation. Electron density and temperature are known to be tightly related like “horse-and-cart”, but in each case it should be specified exactly where the “horse” is and where the “cart” is. According to observations nighttime  $N_mF_2$  enhancements are closely related to the  $h_mF_2$  increases. No  $N_mF_2$  enhancement during quiet time periods has been revealed yet without a corresponding increase in  $h_mF_2$ , while the opposite is possible if the plasmaspheric flux is insufficient (Mikhailov and Förster, 1999). The  $h_mF_2$  increase is produced by the enhanced equatorward thermospheric wind regularly observed in the nighttime  $F_2$ -region (e.g. Buonsanto and Witasse, 1999 and references therein). This  $F_2$ -layer uplift strongly reducing the recombination efficiency, along with usually existing plasma influx from the plasmasphere is the starting point of the nighttime  $N_mF_2$  increasing mechanism. The electron density increase is followed by the electron temperature decrease and corresponding increase in the downward plasma velocity (and flux) resulting in further  $N_e$  increase and so on. Such  $T_e$  and  $V_z$  variations do take place in the Millstone Hill observations (Fig. 6). Therefore, the electron density variation is primary with respect to the electron temperature variation in the scope of the nighttime  $N_mF_2$  increasing mechanism.

This is different from the mechanism of summer evening  $N_mF_2$  enhancement noted by Evans (1965, 1974), and Eccles and Burge (1973) which results from a collapse of the  $F_2$ -layer when the electron temperature decreases at sunset. This produces a strong surge of downward plasma flux into the  $F_2$ -region (Evans, 1974), which along with the  $F_2$ -layer uplifting produces a well-pronounced evening  $N_mF_2$  enhancement (Eccles and Burge, 1973). In this case the electron gas cooling is the primary process with respect to  $N_e$  variations.

In case of the nighttime  $N_mF_2$  enhancements the electron temperature may demonstrate various types of variation, but they are always linked to the  $N_e$  variations, the latter being linked to the  $h_mF_2$  variations (see earlier). Nighttime  $h_mF_2$  variations are known to be due to thermospheric wind and electric field as well as to thermospheric parameter variations, but not to electron temperature. Within the scope of the mechanism considered the  $N_mF_2$  peak occurrence and its timing are mostly determined by  $V_{nx}$  variations, producing the

corresponding  $h_mF_2$  variations. In case of an undeveloped  $h_mF_2$  increase no  $N_mF_2$  enhancement is observed (Fig. 7). The other side of the mechanism is the plasma influx from the plasmasphere. These fluxes are  $(1-2) \times 10^8 \text{ cm}^{-2} \text{ s}^{-1}$  at low and moderate solar activity and up to  $(7-8) \times 10^8 \text{ cm}^{-2} \text{ s}^{-1}$  at solar maximum. It should be stressed that these estimations were made inside the  $F_2$ -region below 450 km where a comparison with the observations was possible while the plasmaspheric fluxes are generally smaller in the upper ionosphere. This is due to a slight variation of the plasma velocity with altitude during nighttime hours (Evans, 1971), therefore the flux should decrease with height (e.g. Evans, 1974). With regard to the solar activity dependence of the plasmaspheric flux it should be kept in mind that vertical plasma velocities are about the same throughout the solar cycle and the plasmaspheric flux increase up to  $(7-8) \times 10^8 \text{ cm}^{-2} \text{ s}^{-1}$  is mostly due to the general increase in the electron density during solar maximum.

The electric field effects were shown to be small at high solar activity on January 27–28, 1990 although the observed  $V_{pn}$  variations were rather strong despite the quiet geomagnetic conditions. Due to the strong anticorrelation between  $V_{pn}$  and  $V_{par}$  plasma moves mostly in the horizontal direction, therefore this motion does not contribute to the  $h_mF_2$  variations and does not help in producing the  $N_mF_2$  increase via this channel. The time-averaged horizontal velocity provides a horizontal plasma influx which is much less than the influx from the plasmasphere.

There is a question concerning the plasma compression/decompression mechanism which allowed us to explain night-to-night  $N_mF_2$  variations during solar minimum in January 1997 (Mikhailov and Förster, 1999), but is not seen to be efficient during solar maximum in January 1990. This may be due to the different plasma filling of the magnetic flux tubes in these two cases. According to Krinberg and Tashchilin (1982) the saturation time is  $T_s \approx 0.17 \times L^4$  days. With  $L = 3.13$  for Millstone Hill, this gives  $T_s \approx 16$  days for such a flux tube. With regard to the January 06–12, 1997 CEDAR period, the last geomagnetic disturbance was two weeks before on December 23, 1996. This is a time interval which is close to  $T_s$  for this magnetic tube which should be practically filled in this case. Therefore, plasma moving under the action of  $\mathbf{E} \times \mathbf{B}$  drift from higher  $L$  shells to lower ones should be squeezed into the  $F_2$ -region providing a sufficient influx to produce the observed  $N_mF_2$  enhancement. Due to low recombination efficiency during solar minimum (see earlier) the required fluxes are rather moderate  $(1-2) \times 10^8 \text{ cm}^{-2} \text{ s}^{-1}$  which are comparable with flux squeezed into the  $F_2$ -region under this compression mechanism (Mikhailov and Förster, 1999). The other period of January 27–28, 1990, took place immediately after a prolonged disturbed period and the magnetic tube should be emptied to a great extent. It may be considered that the plasma compression mechanism under the  $\mathbf{E} \times \mathbf{B}$  drift is not efficient for such magnetic flux tubes.

## Conclusions

The main results of our analysis are the following.

1. A morphological study of the post-midnight  $N_mF_2$  peak occurrence on Boulder ionosonde observations has shown no substantial differences between the Eurasian and the American sectors at least for stations with  $L \approx 3$ . There is a well-pronounced seasonal dependence in the occurrence probability of the peak. Similar to the Eurasian sector, the peak occurs most frequently in winter (November–February 70–80% of all quiet days), while the summer probability is about 40%. The seasonal pattern is about the same regardless of the level of solar activity. Also similar to the Eurasian sector, the winter nighttime enhancements are the largest with amplitudes being larger during solar minimum and with winter peaks being later in local time than the equinoctial and the summer ones. These morphological findings contradict the results of other authors who analyzed this effect in the American sector earlier.

2. The mechanism of winter nighttime  $N_mF_2$  enhancements was considered using Millstone Hill IS radar observations. This mechanism provides consistency with the observations on the set of main parameters. The primary and necessary step in this mechanism is the  $h_mF_2$  increase due to the equatorward thermospheric wind maximizing soon after midnight and lifting the  $F_2$ -layer from the high-recombination area. The downward plasmaspheric flux which always exists during nighttime hours, starts the  $N_mF_2$  increasing process. The electron temperature follows with the opposite sign of the electron density variations in this process. This is a self-supporting avalanche-type process leading to an increase in the downward plasma velocity. The related enhanced plasma influx results in the  $N_mF_2$  increasing. The decrease in the thermospheric wind velocity stops and inverts this process forming the  $N_mF_2$  peak.

3. The amplitude of the  $N_mF_2$  enhancement reflects the balance between plasma influx and the efficiency of recombination in the  $F_2$ -region. Both specific plasma influx and specific number of recombinations increase with solar activity, but the recombination increases faster. The peak value of the downward flux increases by a factor of 4 while the recombination efficiency increases by a factor of 10 when we pass from solar minimum to solar maximum conditions. This explains the decrease in the amplitude of the  $N_mF_2$  peak with solar activity. The crucial factor in this solar activity dependence is the decreased equatorward neutral wind during high solar activity which keeps the  $F_2$ -layer in the high recombination area.

4. The  $\mathbf{E} \times \mathbf{B}$  plasma drift appears to be inefficient for the  $N_mF_2$  nighttime peak formation. On one hand, it has a small effect on the  $h_mF_2$  variation due to strong anticorrelation between  $V_{pn}$  and  $V_{par}$  resulting mainly in the horizontal plasma transfer. On the other hand, this horizontal velocity provides a horizontal plasma influx which is much smaller compared to the influx from the plasmasphere. A similar conclusion on small  $\mathbf{E} \times \mathbf{B}$  drift effects was obtained by Jain and Williams (1984) who analyzed the St. Santin nighttime observations.

5. The plasma compression/decompression mechanism which was useful to explain the night-to-night  $N_m F_2$  variations during solar minimum in January 1997, obviously did not work during high solar activity in January 1990. Different plasma filling of the magnetic flux tubes in these two cases is proposed as a plausible explanation.

*Acknowledgements.* We are grateful to the late Mike Buonsanto and the Millstone Hill Group of the Massachusetts Institute of Technology, Westford, for providing the data. This work was supported by the NATO Collaborative Research Grant EST.CLG 975303.

Topical Editor M. Lester thanks S.A. Gonzalez and N. Jakowski for their help in evaluating this paper.

## References

- Antonova, L. A., V. A. Ershova, G. S. Ivanov-Kholodny, and V. G. Istomin, The  $O^+ - H^+$  transition height and its dependence on solar activity as measured by ACTIVE satellite, *Geomagn. Aeron.*, **32**, 511–514, 1992.
- Arendt, P. R., and H. Soicher, Downward electron flux at 1000 km altitude from electron content measurement at mid-latitudes, *Nature*, **204**, 983–984, 1964.
- Balan, N., and P. B. Rao, Latitudinal variations of nighttime enhancements in total electron content, *J. Geophys. Res.*, **92**, 3436–3440, 1987.
- Banks, P. M., and G. Kockarts, *Aeronomy*, Academic Press, New York, 1973.
- Bertin, F., and J. Papet-Lepine, Latitudinal variation of total electron content in the winter at middle latitude, *Radio Sci.*, **5**, 899–906, 1970.
- Brace, L. H., and R. F. Theis, Global empirical modes of ionospheric electron temperature in the upper F-region and plasmasphere based on in situ measurements from the Atmosphere Explorer-C, ISIS-1 and ISIS-2 satellites, *J. Atmos. Terr. Phys.*, **43**, 1317–1343, 1981.
- Buonsanto, M., Evidence for polarization electric fields in the daytime F region above Millstone Hill, *J. Geophys. Res.*, **99**, 6437–6446, 1994.
- Buonsanto, M., A case study of the ionospheric storm dusk effect, *J. Geophys. Res.*, **100**, 23 857–23 869, 1995.
- Buonsanto, M., and J. M. Holt, Measurements of gradients in ionospheric parameters with a new nine-position experiment at Millstone Hill, *J. Atmos. Terr. Phys.*, **57**, 705–717, 1995.
- Buonsanto, M., and O. G. Witasse, An updated climatology of thermospheric neutral winds and F region ion drifts above Millstone Hill, *J. Geophys. Res.*, **104**, 24 675–24 687, 1999.
- Buonsanto, M. J., and J. C. Foster, Effects of magnetospheric electric fields and neutral winds on the low-middle latitude ionosphere during the March 20–21, 1990, storm, *J. Geophys. Res.*, **98**, 19 133–19 140, 1993.
- Da Rosa, A. V., and F. L. Smith, Behavior of the nighttime ionosphere, *J. Geophys. Res.*, **72**, 1829–1836, 1967.
- Davies, K., D. N. Anderson, A. K. Paul, W. Degenhardt, G. K. Hartmann, and R. Leitinger, Nighttime increase in total electron content observed with the ATS 6 radio beacon, *J. Geophys. Res.*, **84**, 1536–1542, 1979.
- Eccles, D., and J. D. Burge, The behaviour of the upper ionosphere over North America at sunset, *J. Atmos. Terr. Phys.*, **35**, 1927–1934, 1973.
- Evans, J., Observation of F region vertical velocities at Millstone Hill. 1. Evidence for drifts due to expansion, contraction, and winds, *Radio Sci.*, **6**, 609–626, 1971.
- Evans, J., *Technical report 513. Millstone Hill Thomson scatter results for 1969*, Institute of Technology, Lexington, Massachusetts, 1974.
- Evans, J., A study of F2 region night-time vertical ionization fluxes at Millstone Hill, *Planet. Space Sci.*, **23**, 1611–1623, 1975.
- Evans, J., B. A. Emery, and J. M. Holt, *Technical report 528. Millstone Hill Thomson scatter results for 1971*, Institute of Technology, Lexington, Massachusetts, 1978.
- Evans, J. V., Cause of midlatitude winter night increase in  $f_o F_2$ , *J. Geophys. Res.*, **70**, 4331–4345, 1965.
- Förster, M., and N. Jakowski, Interhemispheric ionospheric coupling at the American sector during low solar activity II. Modelling, *Gerlands Beitr. Geophys.*, **95**, 228, 1986.
- Förster, M., and N. Jakowski, The nighttime winter anomaly (NWA) effect in the American sector as a consequence of interhemispheric ionospheric coupling, *PAGEOPH*, **127**, 447–471, 1988.
- Förster, M., V. V. Mikhailov, A. V. Mikhailov, and J. Smilauer, A theoretical interpretation of ion composition measured on board the “Active” satellite in the European sector during April 10–12, 1990 geomagnetic storm, *Ann. Geophysicae*, **13**, 608–616, 1995.
- Hierl, P. M., I. Dotan, J. V. Seeley, J. M. Van Doren, R. A. Morris, and A. A. Viggiano, Rate constants for the reactions of  $O^+$  with  $N_2$  and  $O_2$  as a function of temperature (300–1800 K), *J. Chem. Physics*, **106**, 3540–3544, 1997.
- Jain, A. R., and P. J. S. Williams, The maintenance of the nighttime ionosphere at mid-latitudes, II. The ionosphere above St. Santin, *J. Atmos. Terr. Phys.*, **46**, 83–89, 1984.
- Jakowski, N., and M. Förster, About the nature of the nighttime winter anomaly effect, *Planet. Space Sci.*, **43**, 603–612, 1995.
- Jakowski, N., M. Förster, B. Lazo, and L. Lois, Interhemispheric ionospheric coupling at the American sector during low solar activity I. Observations, *Gerlands Beitr. Geophys.*, **95**, 219–227, 1986.
- Jakowski, N., A. Jungstand, L. Lois, and B. Lazo, Night-times enhancements of the F2-layer ionization over Havana, Cuba, *J. Atmos. Terr. Phys.*, **53**, 1131–1138, 1991.
- Joshi, H. P., and K. N. Iyer, On nighttime anomalous enhancement in ionospheric electron content at lower mid-latitude during solar maximum, *Ann. Geophysicae*, **8**, 53–58, 1990.
- Kersley, L., J. Aarons, and J. A. Klobuchar, Nighttime enhancements in total electron content near Arecibo and their association with VHF scintillations, *J. Geophys. Res.*, **85**, 4241–4222, 1980.
- Krinberg, I. A., and A. V. Tashchilin, Refilling of geomagnetic force tube with a thermal plasma after magnetic disturbances, *Ann. Geophysicae*, **38**, 25–32, 1982.
- Leitinger, R., C. N. Mitchell, L. Kersley, and E. Feichter, On the shape of the winter nighttime trough under quiet geomagnetic conditions, in *Proc. COST-251 Workshop*, Ed. A. Vernon, Funchal, Madeira, Portugal, 123–127, 1999.
- MacPherson, B., S. A. Gonzales, G. J. Bailey, R. J. Moffett, and M. P. Sulzer, The effects of meridional neutral winds on the  $O^+ - H^+$  transition altitude over Arecibo, *J. Geophys. Res.*, **103**, 29 183–29 198, 1998.
- Mahajan, K. K., and O. P. Saxena, Continuous measurements of nighttime electron concentration profiles and estimation of neutral wind velocities at Arecibo, *J. Geophys. Res.*, **81**, 3165–3170, 1976.
- McFarland, M., D. L. Albritton, F. C. Fehsenfeld, E. E. Ferguson, and A. L. Schmeltekopf, Flow-drift technique for ion mobility and ion-molecular reaction rate constant measurements. II. Positive ion reactions of  $N^+$ ,  $O^+$ , and  $N_2^+$  with  $O_2$  and  $O^+$  with  $N_2$  from thermal to 2 eV, *J. Chem. Phys.*, **59**, 6620–6628, 1973.
- Mikhailov, A. V., and M. Förster, Some  $F_2$ -layer effects during the January 06–11, 1997 CEDAR storm period as observed with the Millstone Hill incoherent scatter facility, *J. Atmos. Solar-Terr. Phys.*, **61**, 249–261, 1999.
- Mikhailov, A. V., and K. Schlegel, Self-consistent modelling of the daytime electron density profile in the ionospheric F-region, *Ann. Geophysicae*, **15**, 314–326, 1997.
- Mikhailov, A. V., and K. Schlegel, A self-consistent estimate of  $O^+ + N_2$  rate coefficient and total EUV solar flux with

- $\lambda < 105$  nm using EISCAT observations, *Ann. Geophysicae*, **18**, 2000 (in press).
- Mikhailov, A. V., T. Y. Leschinskaya, and M. Förster**, Morphology of  $N_mF_2$  nighttime increases in the Eurasian sector, *Ann. Geophysicae*, **18**, 618–628, 2000.
- Nusinov, A. A.**, Models for prediction of EUV and X-ray solar radiation based on 10.7-cm radio emission, in *Proc. Workshop on Solar Electromagnetic Radiation Study for Solar Cycle 22*, SEL NOAA ERL, 354–359, 1992.
- Nusinov, A. A., L. A. Antonova, and V. V. Katushina**, Solar fluxes in the 10- to 30-nm range according to studies of the E region and the interlayer ionization valley, *Int. J. Geomag. Aeronom.*, **1**, 153–156, 1999.
- Richards, P. G. et al.**, On the relative importance of convection and temperature to the behavior of the ionosphere in North America during January 6–12, 1997, *J. Geophys. Res.*, **105**, 12763–12776, 2000.
- Standley, P. J., and P. J. S. Williams**, The maintenance of the nighttime ionosphere at mid-latitudes, I. The ionosphere above Malvern, *J. Atmos. Terr. Phys.*, **46**, 73–81, 1984.
- Titheridge, J.**, Nighttime changes in the electron content of the ionosphere, *J. Geophys. Res.*, **73**, 2985–2993, 1968.
- Titheridge, J.**, The electron content of the southern mid-latitude ionosphere, *J. Atmos. Terr. Phys.*, **35**, 981–1001, 1973.
- Torr, M. R., D. G. Torr, R. A. Ong, and H. E. Hinteregger**, Ionization frequencies for major thermospheric constituents as a function of solar cycle 21, *Geophys. Res. Lett.*, **6**, 771–777, 1979.
- Tyagi, T. R.**, Electron content and its variation over Lindau, *J. Atmos. Terr. Phys.*, **36**, 475–487, 1974.
- Young, D. M. L., P. C. Yuen, and T. H. Roelofs**, Anomalous nighttime increases in total electron content, *Planet. Space Sci.*, **18**, 1163–1179, 1970.